Electrostatic forward-viewing scanning probe for Doppler optical coherence tomography using a dissipative polymer catheter

Nigel R. Munce,[1,2] Adrian Mariampillai,[1] Beau A. Standish,[1] Mihaela Pop,[1,2] Kevan J. Anderson,[1,2] George Y. Liu,[1] Tim Luk,[1] Brian K. Courtney,[2] Graham A. Wright,[1,2] I. Alex Vitkin,[1,3,4] and Victor X. D. Yang[2,5,*]

[1]*Department of Medical Biophysics, University of Toronto, 610 University Avenue, Toronto, Ontario M5G 2M9, Canada*
[2]*Imaging Research, Sunnybrook Health Sciences Centre, 2075 Bayview Avenue, Toronto, Ontario M4N 3M5, Canada*
[3]*Ontario Cancer Institute/University Health Network, 610 University Avenue, Toronto, Ontario M5G 2M9, Canada*
[4]*Department of Radiation Oncology, University of Toronto, 610 University Avenue, Toronto, Ontario M5G 2M9, Canada*
[5]*Department of Electrical and Computer Engineering, Ryerson University, 350 Victoria Street, Toronto, Ontario M5B 2K3, Canada*
[*]*Corresponding author: vyang@ee.ryerson.ca*

Received December 14, 2007; accepted January 31, 2008;
posted February 13, 2008 (Doc. ID 90794); published March 21, 2008

A novel flexible scanning optical probe is constructed with a finely etched optical fiber strung through a platinum coil in the lumen of a dissipative polymer. The packaged probe is 2.2 mm in diameter with a rigid length of 6 mm when using a ball lens or 12 mm when scanning the fiber proximal to a gradient-index (GRIN) lens. Driven by constant high voltage (1–3 kV) at low current (<5 μA), the probe oscillates to provide wide forward-viewing angle (13° and 33° with ball and GRIN lens designs, respectively) and high-frame-rate (10–140 fps) operation. Motion of the probe tip is observed with a high-speed camera and compared with theory. Optical coherence tomography (OCT) imaging with the probe is demonstrated with a wavelength-swept source laser. Images of an IR card as well as *in vivo* Doppler OCT images of a tadpole heart are presented. This optomechanical design offers a simple, inexpensive method to obtain a high-frame-rate forward-viewing scanning probe.

OCIS codes: 110.4500, 170.0170, 170.3340, 170.4500, 120.3890.

Catheter-based optical coherence tomography (OCT) has shown promise in diagnosing lesions in both the gastrointestinal [1] and cardiovascular systems [2]. With the advent of frequency domain OCT systems with frame rates exceeding 100 frames/s [3], new optical probes for *in vivo* applications are required to fully capitalize on the benefit of these imaging speed capabilities. Side-viewing rotary probes based on fiber-optic rotary joints have been the workhorse of endoscopic and intravascular OCT systems owing to their high frame rate, minimal sensitivity to turns along the probe's length, and relatively simple implementation. While this imaging geometry is ideal for pullback-style surveys, forward-looking devices may be more amenable to providing interventional guidance. Several groups have proposed different forward-looking strategies for OCT probes based on electroactive polymers [4], fiber bundles [5], piezoelectric scanning [6] and piezoelectric-induced resonance [7], microelectromechanical systems [8,9], and counter-rotating graded-index (GRIN) lenses [10]. The dimensions of the rigid proximal end combined with packaging issues and overall probe complexity are the main difficulties in achieving a low-cost, single-use probe design for use in catheter-based forward-viewing systems *in vivo*. Electrostatic actuation of optical fibers has previously been implemented for optical switches [11]. The inherent rigidity, however, of standard 9/125 single-mode fiber typically necessitates long (~3 cm) cantilever lengths and/or high field strengths in order to obtain relatively small (~200 μm) lateral displacements at the tip.

In this Letter, we implement an electrostatically driven cantilever within a catheter to create a compact, wide-angle, rapid-scanning forward-viewing probe. The novel approach is the use of an electrostatic dissipative plastic to allow the cantilever to oscillate under constant voltage. A schematic of the probe is shown in Fig. 1(a). To increase flexibility, the cladding of a single-mode fiber is etched to 50 μm diameter using a wet-etching technique previously described [12]. The fiber is placed within a 250 μm diameter platinum alloy coil, which is then placed within the 400 μm diameter central lumen of a triple lumen catheter shown in Fig. 1(b). The custom-made catheter is extruded using a dissipative polymer (polyether block amide, Pebax). Dissipative polymers are conductive on the surface only; thus the charge deposited within the material bulk is held for several hundred milliseconds and then migrates to the conductive surface. The two peripheral lumens (diameter 270 μm) contain insulated wires with insulation coatings removed at the cantilever end to provide electrical contact. One of these wires serves as an electrode while the other acts as ground, which are connected to the high voltage (HV) and ground leads of a dc high-voltage power supply, respectively. The current limit of the power supply is set at 20 μA; however, typical currents needed are less than 5 μA.

0146-9592/08/070657-3/$15.00

Fine solder wire is wrapped around the catheter surface and is connected to ground. Initially, the cantilever is neutral and attracted to the HV electrode; however, as it is not directly connected to ground there is no significant electrostatic discharge. When the platinum coil touches the HV electrode, it acquires the same potential. The acquired charge takes a finite time to dissipate through the catheter; during this time the cantilever repels away from the electrode toward the ground wire. When the cantilever touches the ground wire, it becomes neutral again, creating a discharge measurable as a pulse in a parallel circuit located outside of the catheter and serves as a trigger signal for imaging acquisition. As the cantilever returns to ground it is once again attracted to the HV wire, thus creating an oscillating motion.

In one implementation, a 1 mm focal length ball lens is fusion spliced to the distal end of the etched fiber. Alternatively, a 1.8 mm diameter GRIN lens (focal length, 2 mm; pitch, 0.3) is placed in front of the etched fiber to focus the light and amplify the angular displacement of the beam. The small tube can be filled with mineral oil for index matching. The advantage of the GRIN lens is the amplification of the angular displacement of the fiber through the lens; however, it increases the required rigid length from 6 to 12 mm to accommodate the length of the GRIN lens, and it introduces coma aberrations into the image. A photograph of the probe in motion in air outside of the tube is shown in 1(c).

The probe behaves similar to a damped driven oscillator in that there is a certain voltage required to initiate motion. Once the probe begins to oscillate, the voltage may be decreased producing a corresponding decrease in frequency response of the cantilever. The frequency of oscillation as a function of the driving voltage was measured for motion in both air and oil using the frame trigger signal, as shown in Fig. 2(a). For oil immersion, cavitation bubbles were observed at driving high voltages >3.5 kV, 9 μA. The

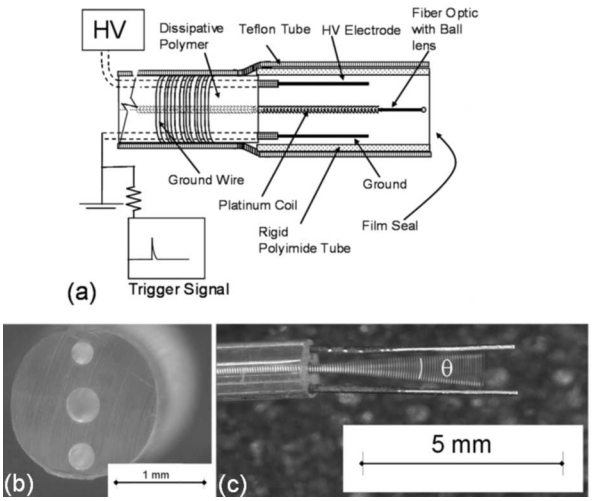

Fig. 1. (a) Schematic of the electrostatic probe, shown with a ball-lensed fiber. (b) End-on view of the three lumen catheter. (c) Photograph of the probe with a ball-lensed fiber within the coil, shown in oscillation driven at 1200 V with 2 μA current. Length of the cantilever was 4 mm with an angle of oscillation $\theta = 13°$.

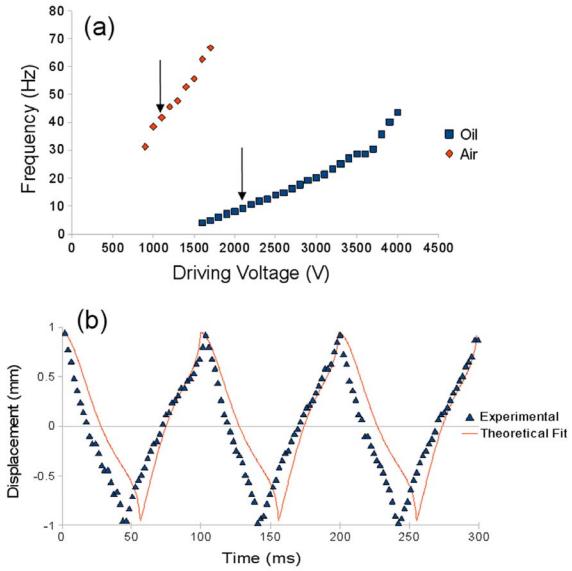

Fig. 2. (Color online) (a) The measured frequency response of the probe as a function of driving voltage in air (diamonds) and mineral oil (squares). Arrows indicate the voltage required to initiate motion. (b) Theoretical model (line) and experimental results (points) of the probe motion. Zero displacement was defined as the midpoint between the two electrodes.

cantilever motion in air exhibited a lower threshold voltage to initiate motion, and a steeper frequency response as compared with the motion in oil. However, slower speeds were possible in oil, which may be advantageous for some imaging applications. In contrast to the frequency response, the amplitude of oscillation is the same in air as in oil, since the cantilever always oscillates between the two electrodes.

We separate the oscillatory motion into an attractive and a repulsive phase and assume that the charge on the cantilever remains constant during one cycle. The attractive phase starts when the cantilever is neutral. We define $r=0$ as the middle of the tube (radius$=R$). The arrangement is modeled as a spring of constant k_s, with a velocity-dependent resistance (proportionality constant α), attracted to a mirror charge q_a, a distance $2(r+R)$ away from the cantilever with Coulomb's electrostatic constant k_c as represented by the third term in the following:

$$\frac{\delta^2 r}{\delta t^2} = -k_s r - \alpha \frac{\delta r}{\delta t} + \frac{k_c q_a^2}{4(r+R)^2}. \quad (1)$$

The repelling phase is when the cantilever has briefly touched the electrode, obtaining some amount of charge (q_b), repelling it from the electrode, as represented by the third term in the following equation; it is also drawn toward the grounding wire owing to the mirror charge effect as represented by the fourth term:

$$\frac{\delta^2 r}{\delta t^2} = -k_s r - \alpha \frac{\delta r}{\delta t} + \frac{k_c q_b q_{elec}}{(r+R)} + \frac{k_c q_b^2}{4(r-R)^2}. \quad (2)$$

In Eq. (2), $k_c q_b^2$ represents the charge on the cantile-

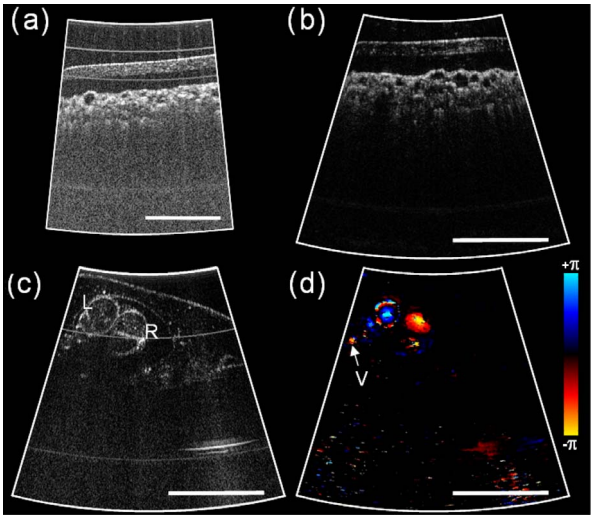

Fig. 3. (Color online) (a) Sector image of an IR card taken using the electrostatic ball-lens probe, resulting in 13° scan angle. (b) Sector image of an IR card taken with an electrostatic probe in which the fiber was scanned behind a GRIN lens, demonstrating 33° scan angle. (c) Structural image of the heart of *Xenopus laevis* taken with the GRIN lens design identifies left (L) and right (R) aortic arches and (d) corresponding Doppler image showing the aortic branches. A small gill vessel is identified with a V. Horizontal scale bars, 1 mm. Scale corresponds to phase shift owing to Doppler effect.

ver and the mirror charge above the ground wire, while q_{elec} represents the electrode charge during repulsion. These two equations can be solved for $r(t)$ to generate a family of triangular waveforms for comparison with experimental measurements. A high-speed CCD camera (MICAM02, BrainVision Inc.) was used to capture images with a temporal resolution of 2.2 ms to analyze in detail the motion of the cantilever. Driving voltage was slowly increased to 2100 V_{DC} such that the probe began to oscillate continuously in mineral oil. The center of the cantilever tip was tracked by software. The results of this motion tracking are shown for three cycles in Fig. 2(b), illustrating a triangular-like waveform at 11 Hz (or 22 fps when both slopes of the triangle are used for imaging). The small difference between theoretical and experimental results is likely caused by the cantilever not being exactly equidistant from the electrode and ground wires at its equilibrium position.

OCT imaging was performed with the prototype probes in the sample arm of a Mach–Zehnder interferometer using a wavelength swept laser centered at 1300 nm with a tuning range of 110 nm and sweeping rate of 43 kHz. In Fig. 3(a) an OCT image of an IR card is shown, acquired with the ball-lens design oscillating at 30 Hz (60 fps) in air with a viewing angle of 13°, while in Fig. 3(b) an OCT image is taken using the GRIN lens probe oscillating at 5 Hz (10 fps) in oil with 33° viewing angle. For Doppler OCT *in vivo* demonstration, we used the GRIN lens electrostatic probe to image the heart of an anesthetized Stage 45 *Xenopus laevus* embryo as shown in Figs. 3(c) and 3(d). These images demonstrate the ability of the probe to generate Doppler images comparable with those obtained with bulk scanning optics.

In conclusion, we have demonstrated a method for rapidly actuating an optical fiber inside a compact catheter in order to obtain forward-viewing OCT images. While high voltage was used to actuate the cantilever, typical currents were ~2 μA. Furthermore, the presence of a ground wire within the catheter and the Teflon tube minimize the chance that a discharge would be delivered to the tissue under examination. The small outer diameter (2.2 mm) and the short rigid length (6 mm) of the probe using the ball-lens design can be further miniaturized to allow for navigating the proximal coronary arteries. While the GRIN lens design has a longer rigid tip section (12 mm) and may not be suitable for the more tortuous sites of the coronary vasculature, the increased angular field of view of this design will likely be useful in other more accessible lumens and orifices of the body. The potential combination of this probe with laser ablation strategies [13] may allow for the application of OCT as an interventional tool in addition to its current diagnostic role, potentially facilitating procedures and expanding the boundaries of minimally invasive interventions.

Support from the Natural Sciences and Engineering Research Council of Canada, Canadian Foundation for Innovation, Ontario Centers of Excellence through the Photonics Research Ontario program, and the Canadian Institutes of Health Research is gratefully acknowledged.

References

1. B. J. Vakoc, M. Shishkov, S. H. Yun, W.-Y. Oh, M. J. Suter, A. E. Desjardins, J. A. Evans, N. S. Nishioka, G. J. Tearney, and B. E. Bouma, Gastrointest. Endosc. **65**, 898 (2007).
2. I. K. Jang, G. J. Tearney, B. MacNeill, M. Takano, F. Moselewski, N. Iftima, M. Shishkov, S. Houser, H. T. Aretz, E. F. Halpern, and B. E. Bouma, Circulation **111**, 1551 (2005).
3. R. Huber, D. C. Adler, and J. G. Fujimoto, Opt. Lett. **31**, 2975 (2006).
4. T. Wang, M. Bachman, G. P. Li, S. Guo, B. J. Wong, and Z. P. Chen, Opt. Lett. **30**, 53 (2005).
5. T. Xie, D. Mukai, S. Guo, M. Brenner, and Z.P. Chen, Opt. Lett. **30**, 1803 (2005).
6. S. A. Boppart, B. E. Bouma, C. Pitris, G. J. Tearney, J. G. Fujimoto, and M. E. Brezinski, Opt. Lett. **22**, 1618 (1997).
7. X. Liu, M. J. Cobb, Y. Chen, M. B. Kimmey, and X. Li, Opt. Lett. **29**, 1763 (2004).
8. J. M. Zara, S. Yazdanfar, K. D. Rao, J. A. Izatt, and S. W. Smith, Opt. Lett. **28**, 628 (2003).
9. T. Xie, H. Xie, G. K. Fedder, and Y. Pan, Appl. Opt. **43**, 6422 (2003).
10. J. Wu, M. Conry, C. Gu, F. Wang, Z. Yaqoob, and C. Yang, Opt. Lett. **31**, 1265 (2006).
11. E. Ollier, P. Labeye, and F. Revol, Electron. Lett. **31**, 2003 (1995).
12. M. Scepanovic, J. E. Castillo, J. K. Barton, D. Mathine, R. K. Kostuk, and A. Sato, Appl. Opt. **43**, 4150 (2004).
13. N. A. Patel, X. D. Li, D. L. Stamper, J. G. Fujimoto, and M. E. Brezinski, Int. J. Cardiovasc. Imaging **19**, 171 (2003).